

Quantum Confinement Effects on Solvatochromic Shifts of Molecular Solutes

Tommaso Giovannini,[†] Matteo Ambrosetti,[‡] and Chiara Cappelli^{*,‡}

[†]*Department of Chemistry, Norwegian University of Science and Technology, 7491*

Trondheim, Norway

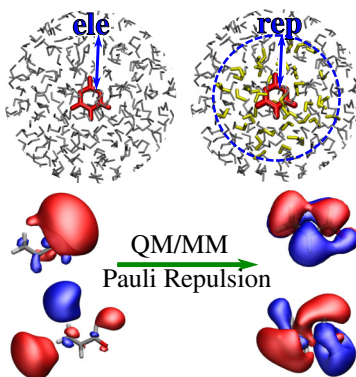
[‡]*Scuola Normale Superiore, Piazza dei Cavalieri 7, 56126 Pisa, Italy.*

E-mail: chiara.cappelli@sns.it

Abstract

We demonstrate the pivotal role of QM density confinement effects on solvatochromic shifts. In particular, by resorting to a QM/MM approach capable of accounting for confinement effects we successfully reproduce vacuo-to-water solvatochromic shifts for dark $n \rightarrow \pi^*$ and bright $\pi \rightarrow \pi^*$ transitions of acrolein and dark $n \rightarrow \pi^*$ transitions of pyridine and pyrimidine without the need of including explicit water molecules in the QM portion. Remarkably, our approach is also able to dissect the effects of the single forces acting on the solute-solvent couple, and allows for a rationalization of the experimental findings in terms of physico-chemical quantities.

TOC graphics



Solvatochromism, i.e. the shift in absorption energies which is evidenced by measuring absorption spectra of a given system as vapor phase or dissolved in a polar solvent, is an amply studied phenomenon.^{1,2} Its rationalization in terms of molecular structural patterns, electronic structure and solute-solvent interactions has benefited much in recent years by the interplay between experiments and computational approaches.³⁻⁸ Due to the nature of solvatochromism, reliable computational methods need to accurately describe the solute’s geometry, but especially its electronic structure both in the ground and excited state(s), which generally means that electron correlation needs to be accounted for. However, the interactions between the solute and the surrounding solvent need to be modeled at the same level of accuracy, so to reproduce all interaction forces between the two players in a physically consistent way.

An iconic case is the vacuo-to-water solvatochromism exhibited by the dark $n \rightarrow \pi^*$ and bright $\pi \rightarrow \pi^*$ transitions of acrolein, which are shifted to opposite directions due to the presence of the surrounding water molecules.^{6,9-14} Different theoretical solvation approaches, either based on purely continuum descriptions¹⁵ or atomistic Quantum Mechanics/Molecular Mechanics (QM/MM)^{16,17} coupled to Molecular Dynamics (MD) simulations, have been challenged to reproduce the experimental findings.^{6,10-14,18-23} While continuum approaches fail, explicit QM/MM methods based either on electrostatic or polarizable schemes, yield computed results in good agreement with respect to experimental values only when explicit water molecules (either 12 or 25)^{10,14} are included in the QM moiety. These findings demonstrate that a proper account of electrostatic interactions is insufficient to reproduce the experimental behavior. In addition, due to the ability of atomistic QM/MM approaches to account for specific (hydrogen bonding) solvent effects, the need to enlarge the QM portion so to include several water molecules clearly shows that solute-solvent non-electrostatic interactions, which are neglected in standard continuum or QM/MM approaches play a crucial role on this property.

In this letter, we demonstrate the pivotal role of QM density confinement effects on sol-

vatochromic shifts. In particular, by resorting to a QM/MM approach able to account for confinement effects we successfully reproduce vacuo-to-water solvatochromic shifts for $n \rightarrow \pi^*$ and bright $\pi \rightarrow \pi^*$ transitions of acrolein and $n \rightarrow \pi^*$ transitions of pyridine and pyrimidine without the need of including explicit water molecules in the QM portion. It is worth remarking that the selected systems present $n \rightarrow \pi^*$ and $\pi \rightarrow \pi^*$ electronic transitions, which are of high chemical interest because among the most common in a plethora of organic molecules. Remarkably, our approach reduces the computational effort required to obtain reliable results and is also capable of dissecting the effects of the single forces acting on the solute-solvent couple, so to allow for a rationalization of the experimental findings in terms of physico-chemical quantities.

The interaction energy $E_{\text{QM/MM}}^{\text{int}}$ between the QM and MM layers within a QM/MM framework can be written as:

$$E_{\text{QM/MM}}^{\text{int}} = E_{\text{QM/MM}}^{\text{ele}} + E_{\text{QM/MM}}^{\text{pol}} + E_{\text{QM/MM}}^{\text{rep}} \quad (1)$$

where $E_{\text{QM/MM}}^{\text{ele}}$ and $E_{\text{QM/MM}}^{\text{pol}}$ are the electrostatic and polarization contributions, respectively. $E_{\text{QM/MM}}^{\text{rep}}$ is Pauli repulsion energy term, which accounts for the QM density confinement. It will be modelled by resorting to the approach which has recently been proposed by some of us,²⁴ and that is able to reproduce intermolecular interaction energies and hyperfine coupling constants of aqueous solutes,²⁵ in almost perfect agreement with full-QM approaches and experiments.²⁴⁻²⁶ Our approach formulates $E_{\text{QM/MM}}^{\text{rep}}$ as the opposite of the exchange integral between QM and MM densities:^{24,27,28}

$$E_{\text{QM/MM}}^{\text{rep}} = \frac{1}{2} \int \frac{d\mathbf{r}_1 d\mathbf{r}_2}{r_{12}} \rho_{\text{QM}}(\mathbf{r}_1, \mathbf{r}_2) \rho_{\text{MM}}(\mathbf{r}_2, \mathbf{r}_1) \quad (2)$$

where (ρ_{QM}) is the QM density, and the MM density (ρ_{MM}) is defined in terms of s-type gaussian functions placed at selected points in the MM portion.²⁴ Coefficients and exponents

of such functions have been determined in a previous work of some of us,²⁴ and successfully coupled to different description of QM/MM coupling.²⁴⁻²⁶ In our approach repulsion affects the molecular density and molecular orbitals, as well as electronic transition energies. Notice that, differently to approximated expressions,²⁹⁻³⁷ the repulsion energy definition in Eq. 2 is formally exact,²⁸ although approximations are introduced in the definition of ρ_{MM} .²⁴ In addition, as it is clear from Eq. 2, its definition is totally independent of the choice of a specific QM/MM approach, and can thus be coupled to any QM/MM description of electrostatic interactions.

Our modeling of repulsion interaction is coupled in this letter with a hierarchy of QM/MM approaches (see Scheme 1) so to finally show that density confinement needs to be included to get a physically consistent picture of solvatochromism. The most basic approach we exploit is the electrostatic QM/MM embedding model (non-polarizable QM/TIP3P³⁸), in which each MM solvent atom is endowed with a fixed charge q . To refine this basic picture, we adopt a polarizable QM/MM based on Fluctuating Charges (FQ),³⁹ in which the charges are not fixed, but can vary as a response to the QM electric potential (as a function of electronegativity, χ , and chemical hardness, η).⁴⁰⁻⁴³ In addition to FQs, in QM/Fluctuating Charges and Fluctuating Dipoles (FQF μ), each MM atom is also endowed with electric dipoles and both charges/dipoles vary as a response to the QM electric potential and field, respectively (as a function of χ , η and polarizability, α).^{26,44,45} Both QM/FQ and QM/FQF μ are based on charge equilibration, thus Charge-Transfer between MM solvent molecules can be allowed (QM/FQ_{CT} and QM/FQF μ _{CT}). In particular, in this work, we allow intermolecular MM CT between water molecules that are placed at a distance lower than 5 Å to any QM atom. The dependence of acrolein excitation energies on the size of the CT region (from 3.5 Å to 8 Å) is reported in Table S1 in the Supporting Information (SI). Notice that charge-equilibration based approaches, such as FQ and FQF μ , suffer from the so-called ‘‘CT catastrophe’’.⁴⁶ For this reason, CT is allowed across a relatively small region (≤ 8 Å). In all calculations, recently reported FQ and FQF μ parametrizations are exploited.^{25,26}

The methodological approach sketched above is applied to QM/MM vertical excitation energies of acrolein, pyridine and pyrimidine in aqueous solution. To this end, in order to account for solvent fluctuations and to sample the phase-space, 100 uncorrelated snapshots were extracted from MD simulations (see Sections S1 and S2.1 given as SI for more details). Vertical excitation energies were also compared with the results obtained by including in the QM portion the water molecules in the first solvation shell (17, 18 and 18 on average for acrolein, pyridine and pyrimidine, respectively), and by treating the remaining solvent molecules with FQ or FQF μ force field (QM/QM_w/FQ and QM/QM_w/FQF μ). Absorption energies were calculated on the same 100 snapshots extracted from MD. The results obtained by exploiting the above super-molecule approaches are taken as a reference (in addition to experiments) to further demonstrate the reliability and robustness of our approach. Notice that the results obtained in this way automatically include Pauli repulsion and intermolecular CT among QM water molecules. Additional calculations at the QM/PCM level, and on full QM clusters (QM-QM_w) made of pyridine+1w (water molecule), acrolein+2w and pyrimidine+2w were also performed.

Let us first focus on the vacuo-to-water solvatochromism exhibited by acrolein. Fig. 1 shows computed vacuo-to-water solvatochromic shifts for the $n \rightarrow \pi^*$ (bottom) and $\pi \rightarrow \pi^*$ (top) transitions of acrolein (the corresponding values are reported in Tab. S2 in SI.).

The bottom part of Fig. 1, reporting the results for $n \rightarrow \pi^*$ transition, shows that the continuum QM/PCM cannot reproduce the vacuo-to-water solvatochromism, whereas the cluster-like QM-QM_w slightly overestimates it. By moving to QM/MM approaches, the non-polarizable QM/TIP3P well reproduces the experimental shift, but the inclusion of Pauli repulsion shifts the computed value to the wrong direction, so that the experimental value is underestimated of 20% (absolute value). A totally different picture is reported for polarizable QM/MM approaches. In fact, both QM/FQ and QM/FQF μ (by either including or neglecting CT effects) overestimate the experimental shift (33% on average). However, similarly to QM/TIP3P, computed vertical transition energies decrease when confinement

(repulsion) effects are considered. Remarkably, the effect of quantum repulsion is substantial, decreasing the solvatochromic shift of 18% on average.

In order to get more insight into the role of repulsion, in Fig. 2 ground and excited state molecular dipole moments are reported (the corresponding data are given in Table S8 in the SI). The reference value for the isolated acrolein at the same level of calculation are 3.5 and 1.0 Debye for ground and $n \rightarrow \pi^*$ excited state, respectively. We see that both the ground and excited states are stabilized by the solvent; however, such a stabilization is larger in case the overall attractive electrostatic solute-solvent interactions are considered. On the other hand, repulsion acts as a confinement of the electron density and therefore the computed dipole moments decrease for all methods. These findings are reflected by computed transition energies (Fig. 1). In fact, the stabilization of the ground state resulting from attractive electrostatic forces, yields a higher transition energy, which is instead reduced when the repulsive term is included. The differences reported by the various polarizable QM/MM approaches are due to a delicate balance between stabilization/destabilization effects of the two (ground/excited) states.

The inclusion of CT effects between MM water molecules has an opposite effect on values computed with QM/FQ or QM/FQF μ . In fact, solvatochromic shift decreases and shifts towards the experiment of almost 15% for QM/FQ_{CT}, whereas it increases (and shifts towards the supermolecule QM/QM_w/MM value) for QM/FQF μ _{CT}. Such an opposite behavior can be rationalized once again by looking at excited state dipole moments (Fig. 2), which decrease moving from QM/FQ to QM/FQ_{CT}, whereas the opposite trend is reported moving from QM/FQF μ to QM/FQF μ _{CT}. This means that in the first case (QM/FQ) the intermolecular CT acts as repulsive force, whereas in QM/FQF μ its effects is to stabilize the excited state. Thus, the larger vacuo-to-water solvatochromism shown by QM/FQF μ is primarily due to a greater stabilization of the ground state with respect to the $n \rightarrow \pi^*$ excited state.

Experimental values are exactly reproduced by QM/FQ_{CT}+rep and QM/FQF μ +rep, whereas

they are overestimated (in absolute value) by QM/FQ+rep and QM/FQF μ_{CT} +rep.

We now move to the bright $\pi \rightarrow \pi^*$ transition of acrolein. The results depicted in Fig. 1 (top) show that both QM/PCM and cluster-like QM-QMw approach cannot properly model this transition. The same applies to QM/TIP3P, which totally fails to reproduce the experiment, giving an error of 44% and exceedingly 67% if repulsion effects are considered.

The results obtained in case of polarizable QM/MM approaches retrace those already discussed for the dark transition, with QM/FQ $_{CT}$ giving a perfect agreement with the experiment when confinement effects are included; again, QM/FQF μ_{CT} +rep shows the best agreement with QM/QM $_w$ /MM solvatochromic shifts. The effect of Pauli repulsion is in this case larger than for $n \rightarrow \pi^*$ transition, with a contribution that reaches 41% in case of QM/TIP3P. It is worth noticing that in this case confinement effects act in opposite direction with respect to $n \rightarrow \pi^*$ excitation. These findings may be explained by the fact that in case of $\pi \rightarrow \pi^*$ transition, the destabilization of the excited state due to the density confinement is predominant with respect to that of the ground state (see also dipole moment values reported in Table S8 in the SI, which confirm this trend); therefore, excitation energies shift to higher values.

Remarkably, the role of MM intermolecular CT effects is opposite with respect to the dark $n \rightarrow \pi^*$ transition; also, such effects seem to be crucial, shifting the values of 35%, on average. In fact, the overall effect of CT is to stabilize the excited state for QM/FQ and QM/FQF μ calculations, thus resulting in larger vacuo-to-water solvatochromism. Therefore, Pauli repulsion and intermolecular CT act for this transition in opposite directions, so that their effects tend to cancel out (see Fig. 1 (top) and Fig. 2). We also note that CT effects are formulated in FQ and FQF μ in a similar way. Numerical differences are hidden in the actual numerical values of the elements of the linear equations that need to be solved (see Refs.²⁶ and⁴¹). For this reason, the numerical entity of CT and electrostatic interactions is difficult to quantify.

To end the discussion on acrolein, in Fig. 3, 12 selected molecular orbitals (both occupied

and virtual) of a randomly selected snapshot extracted from the MD are depicted. Both molecular orbitals obtained by either including or discarding Pauli repulsion are considered. As it is evident, the impact of quantum confinement on molecular orbitals is impressive. Also, virtual orbitals (from 17 on) are shrunk when Pauli repulsion is added; therefore, the aqueous solution has, as expected, a confining effect on the QM density. In light of such findings, remarkably our approach has the potentiality to solve some of the common issues related to the study of Rydberg states.

To further demonstrate the reliability and robustness of our approach, it is also applied to pyridine and pyrimidine, of which vacuo-to-water solvatochromism has been investigated both by exploiting QM/continuum and atomistic QM/MM approaches.^{7,44,47-50}

Solvatochromic shifts as obtained by exploiting different computational approaches are shown in Figs. 4 (values are given in Tables S5 and S7 in the SI). Computed data show a similar behaviour as for acrolein. For both molecules, the continuum QM/PCM and the cluster-like approach (QM-QM_w) cannot reproduce experimental data. Therefore, it comes out that the inclusion of a minimal number of water molecules in the QM moiety is not a suitable approach to solvation, because dynamical and bulk effects are inappropriately modeled.

Moving to QM/MM approaches, non-polarizable QM/TIP3P apparently yields solvatochromic shifts in agreement with experiments and QM/QM_w/MM data, however the agreement decreases when confinement effects are considered. Both polarizable QM/FQ and QM/FQF μ approaches overestimate solvatochromic shifts, however the inclusion of Pauli repulsion shifts the results towards the experimental values. For all considered approaches, quantum confinement has a disruptive impact on the computed solvatochromisms, shifting the values of almost 30/40% on average. The same trend is also shown by computed dipole moments (see Fig. S4 and Table S8 in the SI). In particular, excited state dipole moments substantially decrease (30% on average) due to Pauli repulsion effects, thus also explaining the reported trends in Fig. 4. Similarly to acrolein $n \rightarrow \pi^*$ transition, also in this case intermolecular CT plays an opposite role in QM/FQ and QM/FQF μ . Again, such findings can be explained by

the destabilization that occurs moving from QM/FQ to QM/FQ_{CT}, in which intermolecular CT has overall a repulsive effect (see Fig. S4 in SI).

To summarize, for pyridine QM/FQ_{CT} is in best agreement with experiments (deviation of 3%), whereas QM/FQF μ (regardless the inclusion of CT effects) shows an almost perfect reproduction of reference calculations. For pyrimidine, the best agreement with the experimental value is shown by QM/FQ (6%), however, due to the error bar associated to experimental data, all polarizable QM/MM approaches (with the only exception of QM/FQF μ) give solvatochromic shifts lying within the experimental error.

To conclude, we have demonstrate the crucial role of QM density confinement on the description of solvatochromic shifts. In particular, our results show that excellent agreement with experimental data, not biased by error cancellation, can be obtained by resorting to QM/MM approaches capable of accounting for quantum confinement effects. Our QM/MM calculations are performed on structures extracted from MD simulations. Therefore, the results depend on the reliability of the force field, and on the quality of the sampling of the MD trajectory, which might be both refined by resorting to QM/MM MD. Our approach differs from alternative formulations of non-electrostatic terms,²⁹ and, remarkably, it is much more general so that it can be coupled to any kind of QM/MM approaches, either based on electrostatic- or polarizable-embedding. Potentially, all scientists interested in performing electronic spectra calculations in solution can couple their favorite QM/MM approach to our model for Pauli repulsion. Remarkably, the proposed modeling is not limited to the description of solvatochromic shift; due to its generality, it paves the way to a reliable and physically-consistent modeling of the properties of systems dominated by quantum confinement effects, such as DNA or proteins.

Supporting Information

Computational protocol and computational details. MD Analysis of Acrolein in aqueous solution. Acrolein, pyridine, pyrimidine ω_0 , LR, cLR transition energies. Data related to Figs. 1-2.

Acknowledgments

We are thankful for the computer resources provided by the high performance computer facilities of the SMART Laboratory (<http://smart.sns.it/>). TG acknowledges Dr. Franco Egidi (SNS) for helpful discussion and comments on the manuscript. TG acknowledges funding from the Research Council of Norway through its grant TheoLight (grant no. 275506)

References

- (1) Reichardt, C. Solvatochromism, thermochromism, piezochromism, halochromism, and chiro-solvatochromism of pyridinium N-phenoxide betaine dyes. *Chem. Soc. Rev.* **1992**, *21*, 147–153.
- (2) Reichardt, C. Solvatochromic dyes as solvent polarity indicators. *Chem. Rev.* **1994**, *94*, 2319–2358.
- (3) Loco, D.; Polack, É.; Caprasecca, S.; Lagardere, L.; Lipparini, F.; Piquemal, J.-P.; Mennucci, B. A QM/MM approach using the AMOEBA polarizable embedding: from ground state energies to electronic excitations. *J. Chem. Theory Comput.* **2016**, *12*, 3654–3661.
- (4) Lin, Y.-l.; Gao, J. Solvatochromic shifts of the $n \rightarrow \pi^*$ transition of acetone from steam vapor to ambient aqueous solution: a combined configuration interaction QM/MM simulation study incorporating solvent polarization. *J. Chem. Theory Comput.* **2007**, *3*, 1484–1493.
- (5) Guido, C. A.; Knecht, S.; Kongsted, J.; Mennucci, B. Benchmarking time-dependent density functional theory for excited state geometries of organic molecules in gas-phase and in solution. *J. Chem. Theory Comput.* **2013**, *9*, 2209–2220.

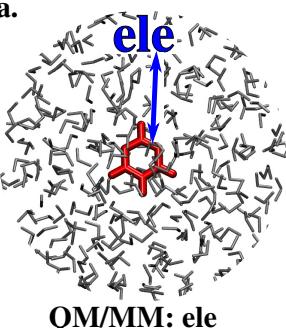
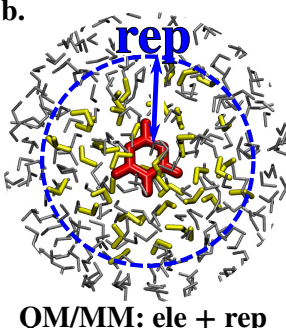
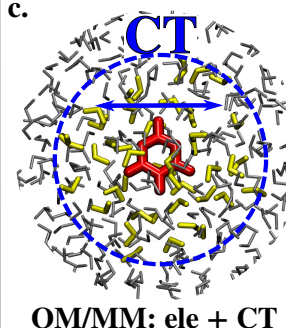
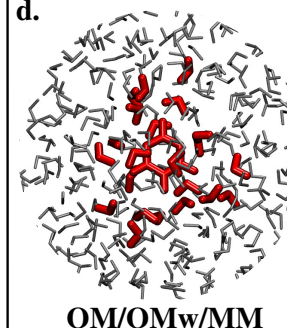
- (6) Marenich, A. V.; Cramer, C. J.; Truhlar, D. G.; Guido, C. A.; Mennucci, B.; Scalmani, G.; Frisch, M. J. Practical computation of electronic excitation in solution: vertical excitation model. *Chem. Sci.* **2011**, *2*, 2143–2161.
- (7) Marenich, A. V.; Cramer, C. J.; Truhlar, D. G. Electronic absorption spectra and solvatochromic shifts by the vertical excitation model: solvated clusters and molecular dynamics sampling. *J. Phys. Chem. B* **2015**, *119*, 958–967.
- (8) Zuehlsdorff, T. J.; Isborn, C. M. Modeling absorption spectra of molecules in solution. *Int. J. Quantum Chem.* **2019**, *119*, e25719.
- (9) Moskvina, A.; Yablonskii, O.; Bondar, L. An experimental investigation of the effect of alkyl substituents on the position of the K and R absorption bands in acrolein derivatives. *Theor. Exp. Chem.* **1966**, *2*, 469–472.
- (10) Aidas, K.; Møgelhøj, A.; Nilsson, E. J.; Johnson, M. S.; Mikkelsen, K. V.; Christiansen, O.; Söderhjelm, P.; Kongsted, J. On the performance of quantum chemical methods to predict solvatochromic effects: The case of acrolein in aqueous solution. *J. Chem. Phys.* **2008**, *128*, 194503.
- (11) Aquilante, F.; Barone, V.; Roos, B. O. A theoretical investigation of valence and Rydberg electronic states of acrolein. *J. Chem. Phys.* **2003**, *119*, 12323–12334.
- (12) Brancato, G.; Rega, N.; Barone, V. A quantum mechanical/molecular dynamics/mean field study of acrolein in aqueous solution: Analysis of H bonding and bulk effects on spectroscopic properties. *J. Chem. Phys.* **2006**, *125*, 164515.
- (13) Duchemin, I.; Guido, C. A.; Jacquemin, D.; Blase, X. The Bethe–Salpeter formalism with polarisable continuum embedding: reconciling linear-response and state-specific features. *Chem. Sci.* **2018**, *9*, 4430–4443.
- (14) Bistafa, C.; Modesto-Costa, L.; Canuto, S. A complete basis set study of the lowest $n-\pi^*$ and $\pi-\pi^*$ electronic transitions of acrolein in explicit water environment. *Theor. Chem. Acc.* **2016**, *135*, 129.

- (15) Tomasi, J.; Mennucci, B.; Cammi, R. Quantum mechanical continuum solvation models. *Chem. Rev.* **2005**, *105*, 2999–3094.
- (16) Warshel, A.; Levitt, M. Theoretical studies of enzymic reactions: dielectric, electrostatic and steric stabilization of the carbonium ion in the reaction of lysozyme. *J. Mol. Biol.* **1976**, *103*, 227–249.
- (17) Senn, H. M.; Thiel, W. QM/MM methods for biomolecular systems. *Angew. Chem. Int. Ed.* **2009**, *48*, 1198–1229.
- (18) Georg, H. C.; Coutinho, K.; Canuto, S. A sequential Monte Carlo quantum mechanics study of the hydrogen-bond interaction and the solvatochromic shift of the $n-\pi^*$ transition of acrolein in water. *J. Chem. Phys.* **2005**, *123*, 124307.
- (19) do Monte, S. A.; Müller, T.; Dallos, M.; Lischka, H.; Diedenhofen, M.; Klamt, A. Solvent effects in electronically excited states using the continuum solvation model COSMO in combination with multireference configuration interaction with singles and doubles (MR-CISD). *Theor. Chem. Acc.* **2004**, *111*, 78–89.
- (20) Martín, M. E.; Muñoz Losa, A.; Fdez.-Galván, I.; Aguilar, M. A theoretical study of solvent effects on the 1 ($n \rightarrow \pi^*$) electron transition in acrolein. *J. Chem. Phys.* **2004**, *121*, 3710–3716.
- (21) Muñoz Losa, A.; Fdez. Galván, I.; Aguilar, M. A.; Martín, M. E. A CASPT2//CASSCF study of vertical and adiabatic electron transitions of acrolein in water solution. *J. Phys. Chem. B* **2007**, *111*, 9864–9870.
- (22) Fukuda, R.; Ehara, M.; Nakatsuji, H.; Cammi, R. Nonequilibrium solvation for vertical photoemission and photoabsorption processes using the symmetry-adapted cluster–configuration interaction method in the polarizable continuum model. *J. Chem. Phys.* **2011**, *134*, 104109.
- (23) Ren, H.; Ming, M.; Zhu, J.; Ma, J.; Li, X. Solvent effect on UV/Vis absorption and emission spectra in aqueous solution based on a modified form of solvent reorganization energy. *Chem. Phys. Lett.* **2013**, *583*, 213–217.

- (24) Giovannini, T.; Lafiosca, P.; Cappelli, C. A General Route to Include Pauli Repulsion and Quantum Dispersion Effects in QM/MM Approaches. *J. Chem. Theory Comput.* **2017**, *13*, 4854–4870.
- (25) Giovannini, T.; Lafiosca, P.; Chandramouli, B.; Barone, V.; Cappelli, C. Effective yet Reliable Computation of Hyperfine Coupling Constants in Solution by a QM/MM Approach: Interplay Between Electrostatics and Non-electrostatic Effects. *J. Chem. Phys.* **2019**, *150*, 124102.
- (26) Giovannini, T.; Puglisi, A.; Ambrosetti, M.; Cappelli, C. Polarizable QM/MM approach with fluctuating charges and fluctuating dipoles: the QM/FQF μ model. *J. Chem. Theory Comput.* **2019**, *15*, 2233–2245.
- (27) Amovilli, C.; Mennucci, B. Self-consistent-field calculation of Pauli repulsion and dispersion contributions to the solvation free energy in the polarizable continuum model. *J. Phys. Chem. B* **1997**, *101*, 1051–1057.
- (28) McWeeny, R. *Methods of molecular quantum mechanics*; Academic press: London, 1992.
- (29) Jensen, J. H.; Gordon, M. S. An approximate formula for the intermolecular Pauli repulsion between closed shell molecules. *Mol. Phys.* **1996**, *89*, 1313–1325.
- (30) Jensen, J. H.; Gordon, M. S. An approximate formula for the intermolecular Pauli repulsion between closed shell molecules. II. Application to the effective fragment potential method. *J. Chem. Phys.* **1998**, *108*, 4772–4782.
- (31) Gordon, M. S.; Freitag, M. A.; Bandyopadhyay, P.; Jensen, J. H.; Kairys, V.; Stevens, W. J. The effective fragment potential method: A QM-based MM approach to modeling environmental effects in chemistry. *J. Phys. Chem. A* **2001**, *105*, 293–307.
- (32) Gordon, M. S.; Slipchenko, L.; Li, H.; Jensen, J. H. The effective fragment potential: a general method for predicting intermolecular interactions. *Annu. Rep. Comput. Chem.* **2007**, *3*, 177–193.
- (33) DeFusco, A.; Minezawa, N.; Slipchenko, L. V.; Zahariev, F.; Gordon, M. S. Modeling solvent effects on electronic excited states. *J. Phys. Chem. Lett.* **2011**, *2*, 2184–2192.

- (34) Slipchenko, L. V. *Many-Body Effects and Electrostatics in Biomolecules*; Pan Stanford, 2016; pp 147–187.
- (35) Gokcan, H.; Kratz, E. G.; Darden, T. A.; Piquemal, J.-P.; Cisneros, G. A. QM/MM Simulations with the Gaussian Electrostatic Model, A Density-Based Polarizable Potential. *J. Phys. Chem. Lett.* **2018**, *9*, 3062–3067.
- (36) Reinholdt, P.; Kongsted, J.; Olsen, J. M. H. Polarizable Density Embedding: A Solution to the Electron Spill-Out Problem in Multiscale Modeling. *J. Phys. Chem. Lett.* **2017**, *8*, 5949–5958.
- (37) Nàbo, L. J.; Olsen, J. M. H.; Holmgaard List, N.; Solanko, L. M.; Wüstner, D.; Kongsted, J. Embedding beyond electrostatics—The role of wave function confinement. *J. Chem. Phys.* **2016**, *145*, 104102.
- (38) Mark, P.; Nilsson, L. Structure and dynamics of the TIP3P, SPC, and SPC/E water models at 298 K. *J. Phys. Chem. A* **2001**, *105*, 9954–9960.
- (39) Rick, S. W.; Stuart, S. J.; Berne, B. J. Dynamical fluctuating charge force fields: Application to liquid water. *J. Chem. Phys.* **1994**, *101*, 6141–6156.
- (40) Lipparini, F.; Cappelli, C.; Barone, V. Linear response theory and electronic transition energies for a fully polarizable QM/classical hamiltonian. *J. Chem. Theory Comput.* **2012**, *8*, 4153–4165.
- (41) Cappelli, C. Integrated QM/Polarizable MM/Continuum Approaches to Model Chiroptical Properties of Strongly Interacting Solute-Solvent Systems. *Int. J. Quantum Chem.* **2016**, *116*, 1532–1542.
- (42) Giovannini, T.; Macchiagodena, M.; Ambrosetti, M.; Puglisi, A.; Lafiosca, P.; Lo Gerfo, G.; Egidi, F.; Cappelli, C. Simulating vertical excitation energies of solvated dyes: From continuum to polarizable discrete modeling. *Int. J. Quantum Chem.* **2019**, *119*, e25684.
- (43) Giovannini, T.; Ambrosetti, M.; Cappelli, C. A polarizable embedding approach to second harmonic generation (SHG) of molecular systems in aqueous solutions. *Theor. Chem. Acc.* **2018**, *137*, 74.

- (44) Giovannini, T.; Riso, R. R.; Ambrosetti, M.; Puglisi, A.; Cappelli, C. Electronic Transitions for a Fully Polarizable QM/MM Approach Based on Fluctuating Charges and Fluctuating Dipoles: Linear and Corrected Linear Response Regimes. *arXiv e-prints* **2019**, arXiv:1906.03852.
- (45) Giovannini, T.; Grazioli, L.; Ambrosetti, M.; Cappelli, C. On the Calculation of IR Spectra with a Fully Polarizable QM/MM Approach Based on Fluctuating Charges and Fluctuating Dipoles. *J. Chem. Theory Comput.* **2019**, DOI: 10.1021/acs.jctc.9b00574.
- (46) Chen, J.; Martínez, T. J. QTPIE: Charge transfer with polarization current equalization. A fluctuating charge model with correct asymptotics. *Chem. Phys. Lett.* **2007**, *438*, 315–320.
- (47) Pagliai, M.; Mancini, G.; Carnimeo, I.; De Mitri, N.; Barone, V. Electronic absorption spectra of pyridine and nicotine in aqueous solution with a combined molecular dynamics and polarizable QM/MM approach. *J. Comput. Chem.* **2017**, *38*, 319–335.
- (48) Biczysko, M.; Bloino, J.; Brancato, G.; Cacelli, I.; Cappelli, C.; Ferretti, A.; Lami, A.; Monti, S.; Pedone, A.; Prampolini, G.; Puzzarini, C.; Santoro, F.; Trani, F.; Villani, G. Integrated computational approaches for spectroscopic studies of molecular systems in the gas phase and in solution: pyrimidine as a test case. *Theor. Chem. Acc.* **2012**, *131*, 1201.
- (49) Cai, Z.-L.; Reimers, J. R. The low-lying excited states of pyridine. *J. Phys. Chem. A* **2000**, *104*, 8389–8408.
- (50) de Almeida, K. J.; Coutinho, K.; De Almeida, W. B.; Rocha, W. R.; Canuto, S. A Monte Carlo–quantum mechanical study of the solvatochromism of pyrimidine in water and in carbon tetrachloride. *Phys. Chem. Chem. Phys.* **2001**, *3*, 1583–1587.

<p>a.</p>  <p>QM/MM: ele</p>	<p>b.</p>  <p>QM/MM: ele + rep</p>	<p>c.</p>  <p>QM/MM: ele + CT</p>	<p>d.</p>  <p>QM/QM_w/MM</p>
<p>MM: TIP3P [q] MM: FQ [q (χ, η)] MM: FQFμ [q, μ (χ, η, α)]</p>	<p>MM: TIP3P [q] MM: FQ [q (χ, η)] MM: FQFμ [q, μ (χ, η, α)]</p>	<p>MM: FQ [q (χ, η)] MM: FQFμ [q, μ (χ, η, α)]</p>	<p>MM: FQ [q (χ, η)] MM: FQFμ [q, μ (χ, η, α)]</p>

Scheme 1: Hierarchy of QM/MM approaches adopted in this work. **a.** electrostatic/polarizable embedding: QM/MM interaction described by means of electrostatic-only terms. **b.** In addition to the electrostatic coupling, Pauli repulsion contribution is considered between the QM solute and the water molecules which are placed at distance lower than 5.0 Å. **c.** Intermolecular CT between solvent water molecules (which are placed at a distance lower than 5.0 Å from the QM) is allowed. **d.** Super-molecule QM/QM_w/MM approach: the first solvation shell (distance lower than 3.5 Å) is included in the QM portion, whereas the remaining solvent molecules are described by means of FQ and FQF μ force fields.

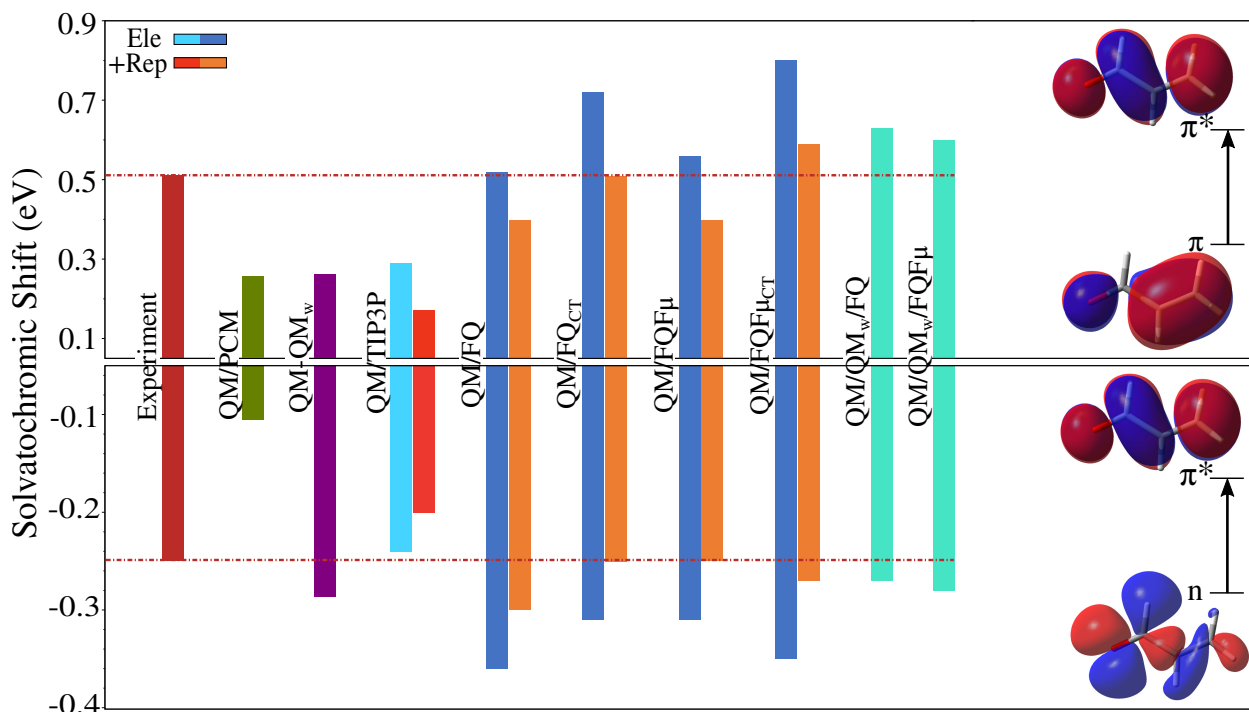


Figure 1: Computed and experimental $n \rightarrow \pi^*$ (bottom) and $\pi \rightarrow \pi^*$ (top) vacuo-to-water solvatochromic shifts of acrolein. Reference computed (CAM-B3LYP/aug-cc-pVDZ) vacuo vertical excitation energies: $n \rightarrow \pi^*$ 3.78 eV (exp.¹⁰ 3.69 eV); $\pi \rightarrow \pi^*$ 6.40 eV (exp.¹⁰ 6.42 eV). Horizontal dashed lines following the experimental data are drawn to guide the eye. Values are given in Table S2 in the SI. All data are reported in eV.

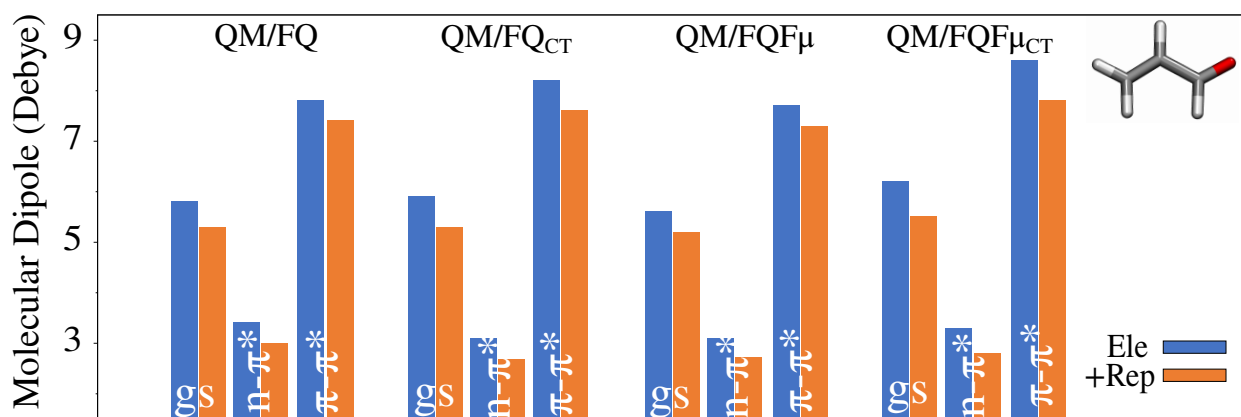


Figure 2: Computed QM/FQ, QM/FQ_{CT}, QM/FQF μ and QM/FQF μ _{CT} acrolein ground and excited state molecular dipole moments. Values are reported in Table S8 in the SI. All data are given in Debye.

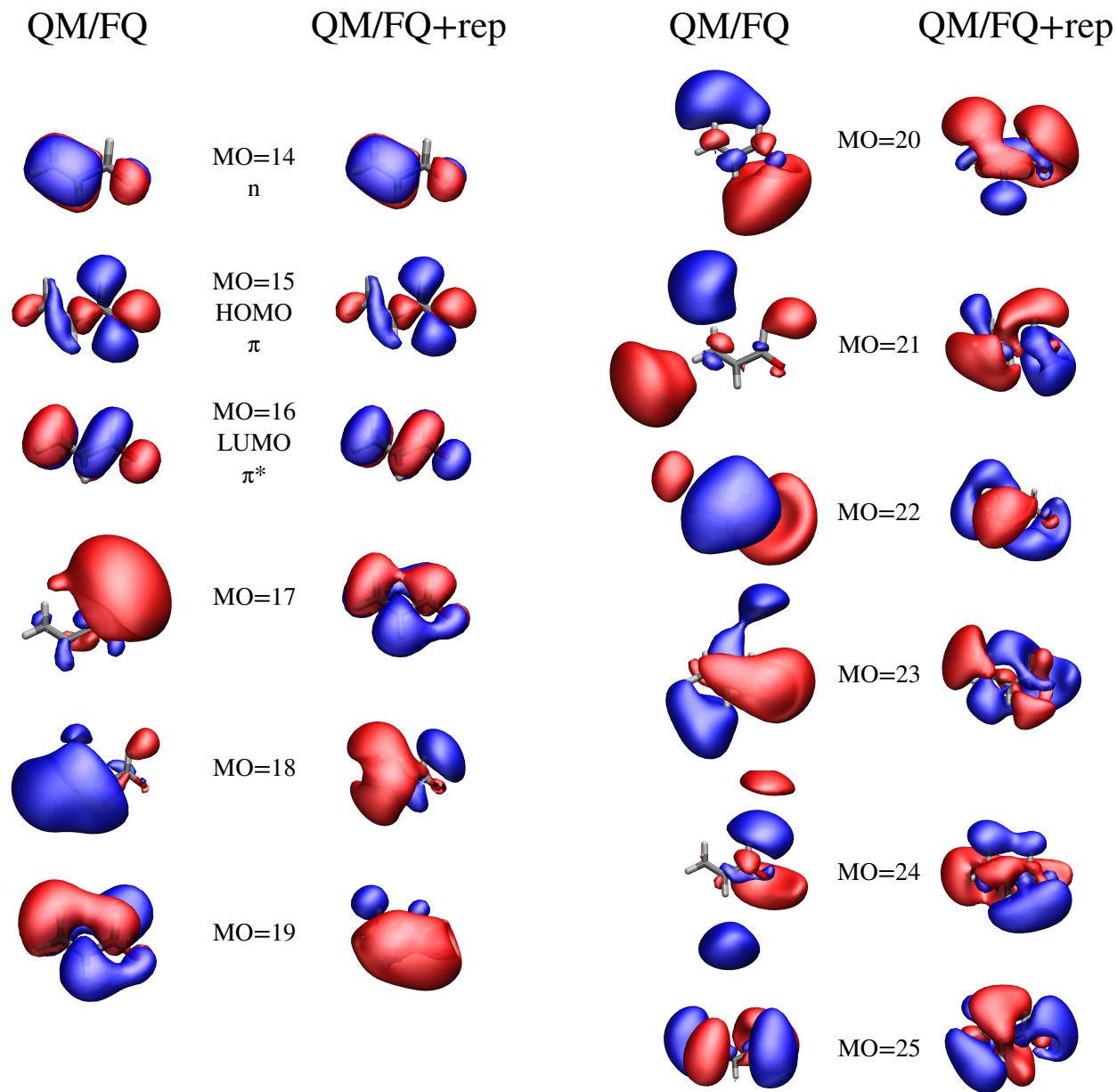


Figure 3: Selected acrolein molecular orbitals for a randomly chosen snapshot extracted from the MD simulation. QM/FQ and QM/FQ+rep values are depicted. Isovalue = 0.02.

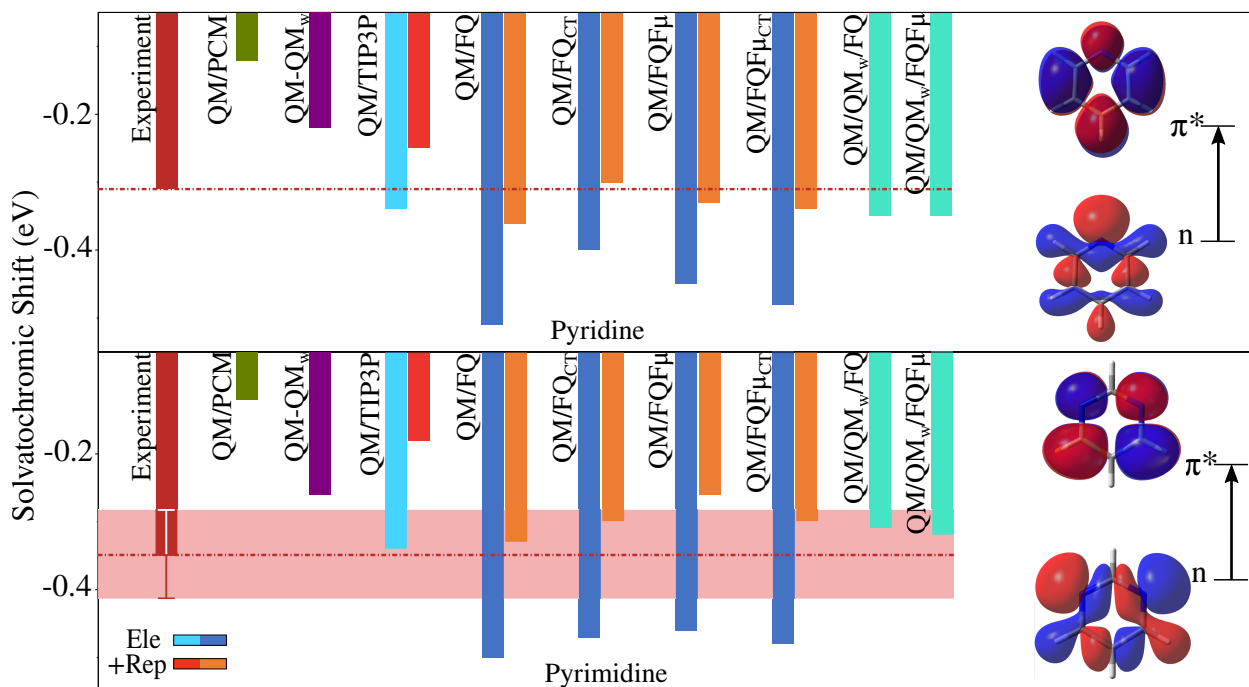


Figure 4: Computed (M06/6-311+G(2df,2p)) and experimental vacuo-to-water solvatochromic shifts for pyridine (top) and pyrimidine (bottom). Reference computed (M06/6-311+G(2df,2p)) vacuo vertical excitation energies: for pyridine $n \rightarrow \pi^*$ 4.67 eV (exp.⁷ 4.63 eV); for pyrimidine $n \rightarrow \pi^*$ 4.17 eV (exp.⁷ 4.18 ± 0.01 eV). Horizontal dashed lines following experimental values are drawn to guide the eye. Values are given in Tables S5 and S7 in the SI. All data are reported in eV.